IOWA STATE UNIVERSITY
Digital Repository

Mechanical Engineering Publications | Mechanical Engineering

5-2015

Quantitative time-averaged gas and liquid distributions using x-ray fluorescence and radiography in atomizing sprays

Christopher D. Radke
NASA-Johnson Space Center

J. Patrick McManamen
NASA-Johnson Space Center

Alan L. Kastengren
Argonne National Laboratory

Benjamin R. Halls
Iowa State University

Terrence R. Meyer
Iowa State University, trm@iastate.edu

Follow this and additional works at: http://lib.dr.iastate.edu/me_pubs

Part of the Aerospace Engineering Commons, and the Mechanical Engineering Commons

The complete bibliographic information for this item can be found at http://lib.dr.iastate.edu/me_pubs/175. For information on how to cite this item, please visit http://lib.dr.iastate.edu/howtocite.html.

This Article is brought to you for free and open access by the Mechanical Engineering at Iowa State University Digital Repository. It has been accepted for inclusion in Mechanical Engineering Publications by an authorized administrator of Iowa State University Digital Repository. For more information, please contact digirep@iastate.edu.

Quantitative time-averaged gas and liquid distributions using x-ray fluorescence and radiography in atomizing sprays

Abstract
A method for quantitative measurements of gas and liquid distributions is demonstrated using simultaneous x-ray fluorescence and radiography of both phases in an atomizing coaxial spray. Synchrotron radiation at 10.1 keV from the Advanced Photon Source at Argonne National Laboratory is used for x-ray fluorescence of argon gas and two tracer elements seeded into the liquid stream. Simultaneous time-resolved x-ray radiography combined with timeaveraged dual-tracer fluorescence measurements enabled corrections for reabsorption of x-ray fluorescence photons for accurate, line-of-sight averaged measurements of the distribution of the gas and liquid phases originating from the atomizing nozzle.

Keywords
absorption, X-ray imaging, fluorescence, synchrotron radiation

Disciplines
Aerospace Engineering | Mechanical Engineering

Comments
This article is from *Optics Letters* 40 (2015): 2029, doi: 10.1364/OL.40.002029. Posted with permission.

Rights
This paper was published in Optics Letters and is made available as an electronic reprint with the permission of OSA. The paper can be found at the following URL on the OSA website: https://www.osapublishing.org/ol/abstract.cfm?uri=ol-40-9-2029&origin=search. Systematic or multiple reproduction or distribution to multiple locations via electronic or other means is prohibited and is subject to penalties under law.

This article is available at Iowa State University Digital Repository: http://lib.dr.iastate.edu/me_pubs/175

Quantitative time-averaged gas and liquid distributions using x-ray fluorescence and radiography in atomizing sprays

Christopher D. Radke,[1,2,*] J. Patrick McManamen,[1] Alan L. Kastengren,[3] Benjamin R. Halls,[2,4] and Terrence R. Meyer[2]

[1]*Propulsion and Power Division, NASA-Johnson Space Center, Houston, Texas 77058, USA*

[2]*Department of Mechanical Engineering, Iowa State University, Ames, Iowa 50011, USA*

[3]*X-Ray Science Division, Argonne National Laboratory, Argonne, Illinois 60439, USA*

[4]*Presently at Air Force Research Laboratory, Aerospace Systems Directorate, Wright-Patterson AFB, Ohio 45433, USA*

**Corresponding author: Christopher.D.Radke@NASA.gov*

Received October 29, 2014; revised March 30, 2015; accepted March 31, 2015; posted April 2, 2015 (Doc. ID 224437); published April 24, 2015

A method for quantitative measurements of gas and liquid distributions is demonstrated using simultaneous x-ray fluorescence and radiography of both phases in an atomizing coaxial spray. Synchrotron radiation at 10.1 keV from the Advanced Photon Source at Argonne National Laboratory is used for x-ray fluorescence of argon gas and two tracer elements seeded into the liquid stream. Simultaneous time-resolved x-ray radiography combined with time-averaged dual-tracer fluorescence measurements enabled corrections for reabsorption of x-ray fluorescence photons for accurate, line-of-sight averaged measurements of the distribution of the gas and liquid phases originating from the atomizing nozzle. © 2015 Optical Society of America

OCIS codes: (010.1030) Absorption; (110.7440) X-ray imaging; (260.2510) Fluorescence; (340.6720) Synchrotron radiation.

http://dx.doi.org/10.1364/OL.40.002029

Efficient injection, atomization, and mixing of the fuel and oxidizer are critical factors influencing combustion stability, performance, and emissions in a variety of devices used for propulsion and power generation [1,2]. To understand and optimize atomization and mixing in many applications, a variety of noninvasive optical measurement techniques have been utilized, such as Mie scattering [3], planar laser-induced fluoresence [4], phase Doppler interferometry [5], and structured laser illumination planar imaging (SLIPI) [6]. Quantitative measurements of breakup characteristics, droplet size, and velocity statistics, and mass distributions using these techniques can provide insight into combustion performance as well as benchmark data necessary to validate empirical and numerical models.

To probe the optically dense, near-nozzle region of the spray, a number of strategies have been developed. Ballistic imaging utilizes spatial, coherence, and time-gated filtering to reduce the signal contribution of diffuse light scattering from the droplet phase. This has allowed interrogation of the spray structure within liquid jets in gaseous crossflows, rocket nozzles, aerated jets, and diesel sprays [7,8]. Techniques based on x-ray radiation from synchrotron and tube sources differ from ballistic imaging in that quantitative measurements of liquid distribution are insensitive to the range of size scales from droplets to liquid core structures. This has allowed investigation of the two- and three-dimensional liquid distribution in atomizing sprays [9–12].

Because x-ray radiography integrates the effects of all attenuating species along the path of the beam, however, it is very difficult to separately identify the distributions of multiple gases or liquids in heterogeneous mixtures. This impedes understanding of gas-liquid mixing under conditions with significant evaporation or for bi-propellant sprays in which either the fuel or oxidizer is delivered as a liquid or gas.

Recently, it has been shown that gas phase concentrations can be measured using x-ray fluorescence [13,14]. In x-ray fluorescence, illumination by x-rays with sufficient energy causes photoionization of an electron in the shell, leading to the emission of x-rays at specific energies associated with an electron filling the vacancy from a nearby shell. X-ray fluorescence can be used to identify specific elements because the fluorescence photon energy is dependent on the atomic number of each element. As such, x-ray fluorescence is sensitive to the density of the targeted element but is insensitive to chemical bonding, pressure, temperature, or physical phase. As the emission is in the x-ray regime, it is not attenuated significantly by scattering from phase interfaces and may be a potentially valuable tool for studying the liquid and/or gas-phase distributions in atomizing sprays.

In the current work, we demonstrate that simultaneous x-ray radiography and x-ray fluorescence can be used to separately measure the gas and liquid phase distributions in bi-propellant atomizing sprays. This is accomplished by introducing a method for simultaneous liquid x-ray fluorescence and gas-phase x-ray fluorescence or radiography for investigating multiphase fuel and oxidizer mixing processes.

The experiments in the current work were conducted utilizing narrowband x-ray radiation from the Advanced Photon Source (APS), 7-BM beamline, at Argonne National Laboratory. In contrast to optical diagnostics utilizing visible light, which can be scattered, refracted or reflected by phase boundaries, low-energy x-rays primarily interact with matter through absorption and weak scattering. Since the refractive index of x-rays is near

 © 2015 Optical Society of America

unity, attenuation is the main effect resulting from the presence of material within the beam path. As such, the attenuation of the x-ray beam through the spray can be related to the path length of the absorbing medium using a constant attenuation coefficient in the Beer–Lambert Law [15]. Even if the material is not isotropic, the Beer–Lambert law applies, keeping in mind that the measured quantity is a pathlength-integrated measure of material density in the beam. Furthermore, the highly collimated, high-photon flux x-ray beams from a synchrotron source enables measurements with high signal-to-noise even for low absorber concentrations [16–19]. This allows for time-resolved radiography without the use of a contrast enhancing agent, and time-averaged x-ray fluorescence can be achieved using small (100 s of ppm) concentrations of tracer species.

The flow geometry, as shown in Fig. 1 (left and middle), is a gas-liquid swirl coaxial injector designed to produce 110 N thrust utilizing liquid oxygen and gaseous methane propellants. In the injector, a centrally located pressure swirl atomizer discharges a hollow cone into a circular annulus of flowing gas. The pressure swirler has an inner diameter of 3.2 mm and an outer diameter of 6.8 mm. The outer diameter of the gas annulus is 10.5 mm, and the distance between the pressure swirl atomizer and the injector exit is 10.2 mm. In the current work, water is used as a simulant for liquid oxygen, and argon is used as a simulant for gaseous methane. Despite the differences between the simulants and the designed fluid, parameters such as momentum ratio between the fluids were maintained near operational conditions.

Volumetric flow meters, pressure transducers, and thermocouples were used to compute state properties. In the current work, the liquid water flow rate was held constant at 1.63 liters per minute (LPM) and the gas was injected at approximately 150 kPa into atmospheric pressure with a volumetric flow rate of 148 LPM.

The x-ray source for the current work is a synchrotron-bending magnet producing a nearly collimated, polychromatic x-ray beam. The beam is then passed through a double-multilayer monochromator ($\Delta E/E = 1.4\%$) to create a monochromatic beam. The beam is then focused using a pair of 300 mm long mirrors in a Kirkpatrick–Baez geometry at 5 mrad grazing angle [20]. The resolution normal to the beam direction was close to the 5 μm × 7 μm full width at half maximum focus of the beam. The divergence of the beam was approximately 2 mrad (vertical) × 3 mrad (horizontal).

As shown in Fig. 1 (right), a silicon drift diode (SDD) integrated the fluorescence signal along the ~1 cm long probe volume at a distance of approximately 15 cm. To reduce slight elastic scattering from the excitation beam, which is comparable to the fluorescence signal but spectrally distinct, the SDD was positioned at approximately 90 degrees and placed behind a Teflon shield. Radiography data were acquired at 1 MHz using a PIN diode with a multipole filter and collected in 2 s exposures on a digital oscilloscope sampling at 6.25 MHz.

For all measurements, the incident x-ray beam was set to 10.1 keV. This energy is low enough to enable significant attenuation in the liquid while also exciting both liquid and gas-phase x-ray fluorescence. To excite liquid fluorescence, 200 ppm of nickel sulfate hexahydrate (7.5 keV Kα, 8.3 keV Kβ) and 200 ppm of zinc sulfate heptahydrate (8.6 keV Kα, 9.6 keV Kβ) were dissolved in water [21]. The liquid properties of the salt solutions were similar to water within the accuracy of the measurements of viscosity (~1%) and surface tension (~3%), using a falling ball rheometer and force tensiometer, respectively. The use of two tracer species allows for correction of fluorescence reabsorption through the spray to an accuracy of approximately 5% [22] by comparing the ratio of detected fluorescence from the two species [23]. If the attenuation from the location of fluorescence signal generation to the detector is large, for example, then the lower energy fluorescence from nickel will be more highly attenuated than that from zinc. Gas phase fluorescence of argon (2.9 keV Kα, 3.2 keV Kβ) [13,21] was collected simultaneously with the liquid phase fluorescence, as shown in Fig. 2. Argon also strongly absorbs x-rays, providing radiography contrast between argon and ambient air. In this manner, the gas-phase distribution can either be measured directly using the argon fluorescence signal (after correction for reabsorption) or by subtracting the liquid path length measured using fluorescence from the total liquid and gas-phase path lengths measured using radiography.

Simultaneous radiography and fluorescence measurements were collected for a given set of flow rates at several locations across the spray. This was accomplished with a fixed x-ray beam path and by traversing the spray through the beam over a transverse extent of −10 mm to 10 mm from the centerline of the injector and at multiple downstream locations. Examples of the raw transmission and fluorescence signals for a transverse scan at 6 mm downstream are shown in Fig. 3. Note that the transmission measured along the beam path is radially symmetric,

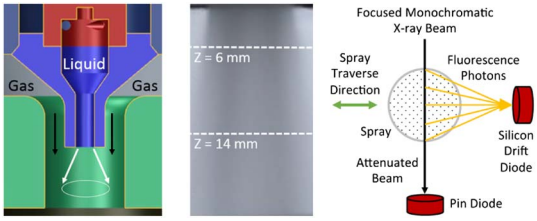

Fig. 1. Cross-section of injector (left), typical visible back-lit image of the spray (middle), and x-ray detection scheme (right).

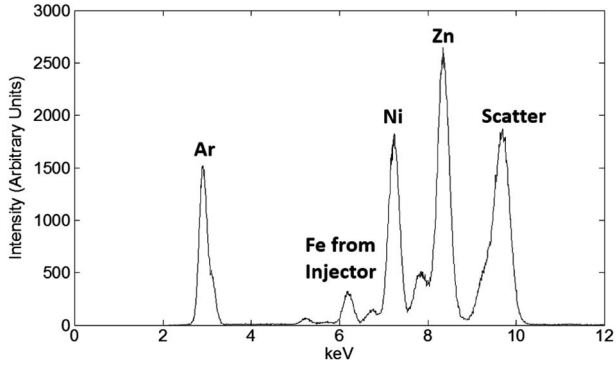

Fig. 2. Example fluorescence spectrum collected from argon gas and Ni-Zn liquid tracers.

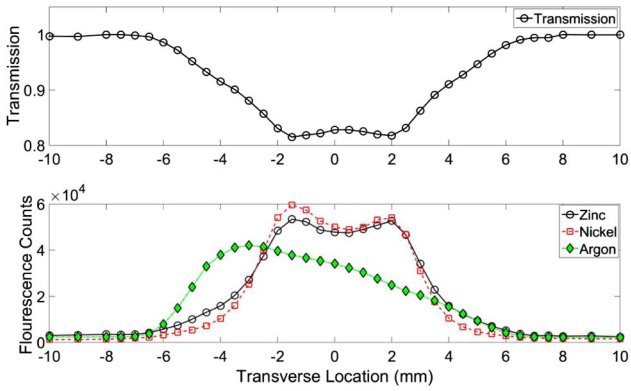

Fig. 3. Raw signal attenuation (top) and uncorrected fluorescence signals (bottom) at $Z = 6$ mm downstream of the injector exit.

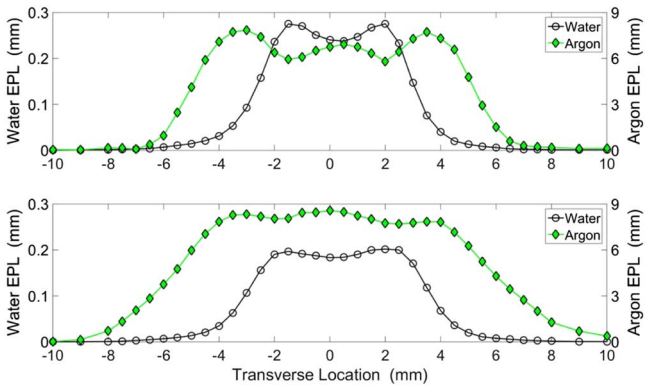

Fig. 4. Equivalent path length profiles at downstream locations of $Z = 6$ mm (top) and $Z = 14$ mm (bottom), as shown in the spray image of Fig. 1.

as expected because of the shape of the spray nozzle, while the fluorescence profiles are suppressed at positive transverse locations because the signals in this region must pass through a larger part of the spray on the path to the SDD. The higher level of reabsorption levels for the argon fluorescence signal was due in part to the geometry of the spray as well as the relatively high absorption coefficient for the argon fluorescence signals at ~3 keV.

To obtain a quantitative measurement of the equivalent path length (EPL) of argon at each transverse location, a multi-step post-processing procedure can be performed to correct for reabsorption similar to that detailed by Lin *et al.* [14]. In the current work, however, the argon EPL was found by an alternative means. The attenuation associated with the liquid phase was first obtained using fluorescence from the nickel and zinc tracers. The liquid attenuation was then subtracted from the total attenuation and was used to calculate the argon EPL using the Beer–Lambert Law. This technique has an advantage in cases where high liquid densities near the injector exit cause substantial trapping of argon fluorescence, leading to significant reabsorption corrections and producing high uncertainties in the argon EPL measurements. In contrast, the relatively more-precise measurement of total-minus-liquid attenuation can be used for accurate measurements even at locations with low argon fluorescence signals caused by low concentrations or high levels of reabsorption.

For the case of liquid fluorescence, two tracer species with differing x-ray fluorescence energies are used to directly infer the amount of reabsorption of the raw signal on the path to the fluorescence detector [22,23]. This is an improvement over previous approaches that utilized radiography alone to measure the liquid distribution, as the total attenuation is affected by the presence of argon. Hence the dual-tracer technique provides an independent means of correcting for both liquid and argon fluorescence reabsorption.

The adjustments for fluorescence reabsorption are also accompanied by corrections to compensate for dead time in the fluorescence photon counting system, variations in the incoming beam intensity, and attenuation of the incident beam and resulting fluorescence signal [24]. Next, fluorescence from the tracer species and attenuation due to water are correlated using a scan without argon flowing. Finally, the water contribution is extracted from the total attenuation, thereby leaving the attenuation and path length associated with argon.

Examples of the corrected argon and liquid distribution profiles are shown in Fig. 4. As noted earlier, the spray is radially symmetric (to within about 1.4%) based on the total transmission through the spray. This is also reflected in the liquid EPL profiles of Fig. 4, with peak values that are symmetric to within 0.1% and 2.5%, respectively, at 6 mm and 14 mm downstream. This is consistent with prior work on dual-tracer x-ray fluorescence reported in literature [22] and implies that accurate absolute liquid EPL values can be obtained through calibration of the corrected liquid fluorescence signals measured without argon flowing. The argon EPL data show slightly higher potential systematic errors, with peak values that are symmetric to within 1.6% and 5%, respectively, at 6 mm and 14 mm downstream. The latter are consistent with dual-tracer liquid fluorescence attenuation corrections reported in prior work [22] and represent systematic errors relative to the attenuation measurements used for calibration of fluorescence signals. The minimum precision of the EPL measurements is 4 μm based on ratios of signal-to-background noise of 83, 260, and 20 for the total, water, and argon EPL data, respectively.

Using this approach, it is possible to probe the interior regions of the spray near the exit plane of the injector and to investigate the relative gas- and liquid-phase distributions. As shown in Fig. 4 (top), the liquid EPL of up to 0.28 mm is distributed over a transverse extent of about 5.5 mm to 6 mm full width at half maximum, which is consistent with a high degree of atomization. It is also observed that the center liquid core is largely surrounded by an outer gas core. Further downstream at 14 mm, the liquid EPL drops, and the profile broadens, indicative of further atomization and mixing. The gas-phase profile also broadens downstream, but in contrast with the liquid-phase, the EPL of the gas-phase appears to increase rather than decrease. The increase in the integrated EPL across the spray at this location is indicative of gas-phase deceleration, while the broadening of the injected gas-phase profile at the exterior of the spray indicates mixing with the ambient gas.

In summary, a new technique for differentiating gas and liquid phases using nonintrusive, synchrotron x-ray radiation has been introduced. By utilizing simultaneous x-ray attenuation and fluorescence of the gas and liquid phases, this technique enables quantitative measurements of the gas and liquid phase distributions within a complex, optically diffuse spray. This approach is sensitive enough to distinguish small changes in the gas-liquid phase distributions that would measurably impact the performance of bipropellant mixing systems. Future work will include measurements using more realistic cryogenic fluids and comparisons with hot-fire test data to evaluate injector performance characteristics.

The work was sponsored by the Propulsion and Power Division at the NASA-Johnson Space Center and by the Army Research Office (Dr. Ralph Anthenien, Program Manager). This research used resources of the Advanced Photon Source, a U.S. Department of Energy (DOE) Office of Science User Facility operated for the DOE Office of Science by Argonne National Laboratory under Contract No. DE-AC02-06CH11357. The authors would like to express gratitude to J.C. Melcher and Robert Morehead for their technical assistance.

References

1. T. R. Meyer, M. Brear, S. H. Jin, and J. R. Gord, in *Handbook of Combustion*, M. Lackner, F. Winter, and A. Agarwal, eds. (Wiley, 2010), pp. 291–322.
2. V. Yang, J. M. Wicker, and M. W. Yoon, Prog. Astronaut. Aeronaut. **169**, 357 (1995).
3. C. F. Bohren and D. R. Huffman, *Absorption and Scattering of Light by Small Particles* (Wiley, 2008).
4. P. Le Gal, N. Farrugia, and D. A. Greenhalgh, Opt. Laser Technol. **31**, 75 (1999).
5. W. D. Bachalo, Appl. Opt. **19**, 363 (1980).
6. E. Berrocal, E. Kristensson, M. Richter, M. Linne, and M. Alden, Opt. Express **16**, 17870 (2008).
7. M. Linne, Prog. Energy Combust. Sci. **39**, 403 (2013).
8. J. B. Schmidt, Z. D. Schaefer, T. R. Meyer, S. Roy, S. A. Danczyk, and J. R. Gord, Appl. Opt. **48**, B137 (2009).
9. B. R. Halls, T. J. Heindel, A. L. Kastengren, and T. R. Meyer, Int. J. Multiphase Flow **59**, 113 (2014).
10. C. J. Eberhart, D. M. Lineberry, R. A. Frederick, Jr., and A. L. Kastengren, J. Propul. Power **30**, 1070 (2014).
11. W. Cai, C. F. Powell, Y. Yue, S. Narayanan, J. Wang, M. W. Tate, M. J. Renzi, A. Ercan, E. Fontes, and S. M. Gruner, Appl. Phys. Lett. **83**, 1671 (2003).
12. M. Linne, Exp Fluids **52**, 1201 (2012).
13. A. L. Kastengren, C. F. Powell, E. M. Dufresne, and D. A. Walko, J. Synchrotron Radiat. **18**, 811 (2011).
14. K. C. Lin, C. Carter, S. Smith, and A. L. Kastengren, in *26th Annual Conference on Liquid Atomization and Spray Systems* (Institute for Liquid Atomization and Spray Systems, 2014).
15. M. J. Berger, J. H. Hubbell, S. M. Seltzer, J. Chang, J. S. Coursey, R. Sukumar, D. S. Zucker, and K. Olsen, XCOM: Photon Cross Sections Database, http://www.nist.gov/pml/data/xcom/
16. S. A. Schumaker, A. L. Kastengren, M. D. Lightfoot, S. A. Danczyk, and C. F. Powell, "A study of gas-centered swirl coaxial injectors using X-ray radiography," in *12th ICLASS*, Heidelberg, Germany (2012).
17. C. F. Powell, Y. Yue, R. Poola, and J. Wang, J. Synchrotron Radiat. **7**, 356 (2000).
18. A. L. Kastengren and C. F. Powell, Proc. Inst. Mech. Eng. Part D **221**, 653 (2007).
19. A. L. Kastengren, C. F. Powell, D. Arms, E. M. Dufresne, H. Gibson, and J. Wang, J. Synchrotron. Radiat. **19**, 654 (2012).
20. P. J. Eng, M. Newville, M. L. Rivers, and S. R. Sutton, Proc. SPIE **3449**, 145 (1998).
21. A. C. Thompson, J. Kirz, D. T. Attwood, E. M. Gullikson, M. R. Howells, J. B. Kortright, Y. Liu, A. L. Robinson, J. H. Underwood, K.-J. Kim, I. Lindau, P. Pianetta, H. Winick, G. P. Williams, and J. H. Scofield, *X-ray Data Booklet* (Lawrence Berkeley National Laboratory, 2009).
22. B. R. Halls, T. R. Meyer, and A. L. Kastengren, Opt. Express **23**, 1730 (2015).
23. A. Kastengren, B. R. Halls, and T. R. Meyer, Bull. Am. Phys. Soc. **58** (2013).
24. D. A. Walko, D. A. Arms, A. Miceli, and A. L. Kastengren, Nucl. Instrum. Methods Phys. Res. Sect. A **649**, 81 (2011).